Letter

Quantum nonlinear metasurfaces from dual arrays of ultracold atoms

Simon Panyella Pedersen,* Lida Zhang (张理达),† and Thomas Pohl‡
Department of Physics and Astronomy, Aarhus University, DK-8000 Aarhus C, Denmark

(Received 14 December 2022; accepted 1 March 2023; published 27 March 2023)

Optical interfaces with subwavelength patterns make it possible to manipulate light waves beyond the typical capabilities of ordinary optical media. Subwavelength arrays of ultracold atoms enable such transformations at very low photon losses. Here, we show how the coupling of light to more than a single atomic array can expand these perspectives into the domain of quantum nonlinear optics. While a single array transmits and reflects light in a highly coherent but largely linear fashion, the combination of two arrays is found to induce strong photon-photon interactions that can convert an incoming classical beam into strongly correlated photonic states. Such quantum metasurfaces open up new possibilities for coherently generating and manipulating nonclassical light, and exploring quantum many-body phenomena in two-dimensional systems of strongly interacting photons.

DOI: 10.1103/PhysRevResearch.5.L012047

Advances in controlling cold atomic ensembles at the single-particle level [1] have enabled the development of novel light-matter interfaces. Recent investigations [2–23] have explored various approaches toward strong and coherent coupling to propagating photons, using nanoscale optical waveguides, photonic crystals, or regularly arranged atoms in free space. In particular, extended two-dimensional lattices of atoms suggest themselves as optical metasurfaces that can be designed and engineered on subwavelength scales at the level of individual quantum emitters. Experiments have demonstrated the strong coherent coupling to subradiant collective excitations of atoms in optical lattices [20], which can enable the near lossless interfacing with a single mode of freely propagating light fields [15–18]. This makes it possible to explore the functionalities of optical metasurfaces [24–28], which, e.g., offers new possibilities for highly coherent wavefront engineering [19]. While dense emitter arrangements with an overall subwavelength dimension can exhibit high nonlinearities akin to a single atom [29,30], the extended geometry of two-dimensional surfaces renders such systems intrinsically linear. In fact, the simultaneous photon interaction with a large number of atoms, necessary to achieve strong collective coupling, diminishes the otherwise strong optical nonlinearity of each individual quantum emitter, thereby, restricting their collective optical response to the domain of linear optics.

Here, we describe and analyze how strong optical nonlinearities can be obtained in metasurfaces composed of subwavelength atomic lattices. Specifically, we will discuss how combining two atomic arrays, which separately are only weakly nonlinear, can greatly enhance their combined optical nonlinearity to a degree that acts on the level of individual photons. The quantum optical nonlinearity in this system

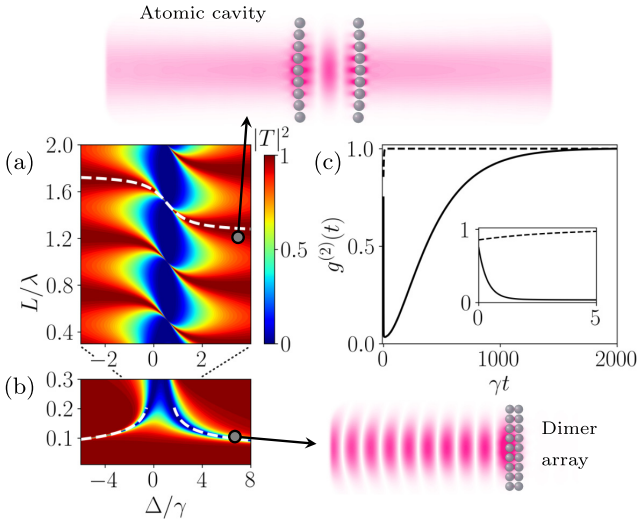

FIG. 1. (a), (b) The transmission spectrum $|T|^2$ of a dual array of two-level emitters exhibits characteristic reflection and transmission resonances as a function of the photon frequency detuning, Δ, and the distance, L, between the two two-dimensional atomic lattices. (b) For small L the system behaves as a single layer of superradiant and subradiant atomic dimers that generate two respective reflection resonances (two white dashed lines). (a) The large-L limit, on the other hand, leads to a series of narrow transmission resonances of the effective atomic resonator (white dashed line) [cf. Eq. (5)]. (c) In the vicinity of such narrow transmission resonances, the optical response becomes highly nonlinear and generates effective photon-photon interactions that can transform an incident coherent beam into highly nonclassical light, as demonstrated by the depicted two-photon correlation function $g^{(2)}(t)$ of the transmitted light (solid line). In contrast, light reflected from a single identical array remains largely uncorrelated (dashed line). The chosen lattice spacing is $a = 0.6\lambda$. The transmission in (a), (b) is obtained for infinite arrays, while the calculations in (c) are for finite arrays with 9×9 atoms driven by a Gaussian laser with a waist of $w = 1.5\lambda$, $\Delta = 0.472\gamma$, and $L = 1.55\lambda$.

*spp@phys.au.dk
†zhanglida@phys.au.dk
‡pohl@phys.au.dk

arises from narrow transmission resonances around which photons are strongly confined between the two arrays, forming a high finesse optical resonator. We show that such dual-array settings can effectively transform an incident classical beam into strongly correlated states of light, while the statistics of incident photons is left virtually unchanged by each individual array [cf. Fig. 1(c)]. The nonlinearity can be traced back to the emergence of an effective photon-photon interaction in the two-dimensional plane of the surface, which is shown to generate in-plane collisions between individual photons. This suggests a promising approach to employing atomic lattices as quantum nonlinear metasurfaces for generating and manipulating nonclassical states of light, and exploring quantum many-body physics with photons [31,32].

Let us first consider a single two-dimensional square lattice of atoms with a lattice spacing a, and which we assume to be infinitely extended in the xy plane. We focus the discussion on two-level systems that are resonantly driven by a coherent cw-field with an electric field amplitude $E_{\rm in}$ and spatial mode function $f(\mathbf{R})$ [33]. At the small lattice spacings considered here, exchange of photons across the array generates strong atomic interactions that can be efficiently described within input-output theory by integrating out the photonic degrees of freedom and using a Born-Markov approximation [34,35]. This yields a master equation $\partial_t\hat{\rho} = -i[\hat{H},\hat{\rho}] + \mathcal{L}[\hat{\rho}]$ (with $\hbar = 1$) for the density matrix, $\hat{\rho}$, of the atomic lattice, where the Hamiltonian and Lindblad operator

$$\hat{H} = -\Delta\sum_n \hat{\sigma}_n^\dagger\hat{\sigma}_n - \sum_n(\Omega_n\hat{\sigma}_n^\dagger + \Omega_n^*\hat{\sigma}_n) - \sum_{n\neq m} J_{nm}\hat{\sigma}_n^\dagger\hat{\sigma}_m, \tag{1a}$$

$$\mathcal{L}[\hat{\rho}] = \sum_{n,m}\Gamma_{nm}(2\hat{\sigma}_n\hat{\rho}\hat{\sigma}_m^\dagger - \{\hat{\sigma}_n^\dagger\hat{\sigma}_m,\hat{\rho}\}), \tag{1b}$$

describe the exchange of excitations and corresponding collective decay processes due to the photon-mediated dipole-dipole interactions between the atoms [36]. Here, $\sigma_n = |g_n\rangle\langle e_n|$ denotes the transition operator between the ground state, $|g_n\rangle$, and excited state, $|e_n\rangle$, of an atom at position $\mathbf{R}_n$ in the lattice. The interaction coefficients J_{nm} and decay rates Γ_{nm} for two atoms at positions $\mathbf{R}_n$ and $\mathbf{R}_m$ are determined by the Green's function tensor of the free-space electromagnetic field [36,37]. The atomic transition is driven by the incident light with a frequency detuning Δ and a single-atom Rabi frequency $\Omega_n = dE_{\rm in}f(\mathbf{R}_n)$, which is determined by the driving-field amplitude and the transition dipole moment d of the two-level emitters. From the solution for $\hat{\rho}$, one can reconstruct the electromagnetic field generated by the driven atomic dipoles. Choosing $f(\mathbf{R}_n)$ as the detection mode for the transmitted light, one obtains [36,37]

$$\hat{E} = E_{\rm in} + i\frac{3\pi\gamma}{k^2\eta d}\sum_n f^*(\mathbf{r}_n)\hat{\sigma}_n \tag{2}$$

for the electric-field amplitude, $\hat{E}$, of the detected photons, where $k = 2\pi/\lambda$ is the wave number of the incident light, λ denotes its wavelength, $\gamma = \Gamma_{nn}$ is the decay rate of the individual atoms, and $\eta = \int d^2r|f(\mathbf{R})|^2$ with $\mathbf{r} = (x,y)$.

For weak plane-wave driving with $f \sim e^{ikz}$, Eqs. (1a), (1b), and (2) yield simple expressions for the transmission and reflection spectra [17]

$$t = \frac{\langle\hat{E}\rangle}{E_{\rm in}}, \quad r = t - 1 = -\frac{i\tilde{\Gamma}}{\Delta - \tilde{\Delta} + i\tilde{\Gamma}} \tag{3}$$

that feature a Lorentzian resonance at the collective Lamb shift $\tilde{\Delta} = -\sum_{n\neq 0}J_{n0}$ with a width $\tilde{\Gamma} = 3\pi\gamma/k^2a^2$. On resonance, the single atomic layer thus reflects incoming photons with unit efficiency and no losses from the incident mode, $|t|^2 + |r|^2 = 1$.

Such high reflectivities are attainable already for remarkably small systems [15]. For example, a 9×9 atomic array with $a = 0.6\lambda$ can reflect into the incident mode of a focused Gaussian beam with a waist of $w = 1.5\lambda$ with a large reflection amplitude of $|r| = 0.998$. On the other hand, the nonlinear response is very small as the beam still covers a sizable number of atoms, which substantially diminishes saturation effects. This is seen directly from the second order correlation function $g^{(2)}(t)$ of the reflected light, shown by the dashed line in Fig. 1(b). Here, one finds only a marginal suppression of simultaneous two-photon reflection, indicating that the reflected light largely retains the classical coherent-state nature of the incident beam ($g^{(2)} \sim 1$).

This situation changes dramatically as we add a second atomic array. Figure 1(a) shows the transmission coefficient $|T|^2$ for a dual-array configuration of two parallel atomic lattices as a function of the detuning Δ and the distance L between the two arrays. The calculations reveal a series of narrow transmission resonances that extends towards large values of L and a pair of sharp reflection resonances at small array distances. Both regimes can be traced back to the photon-mediated interactions between the two arrays.

For small distances L, atoms in different arrays interact via a dipole-dipole coupling that scales as $J_L \approx -3\gamma/2(kL)^3$ [37]. We can, thus, define symmetric and antisymmetric superposition states, $|\pm\rangle_n$, of a single excitation that is symmetrically ($|+\rangle_n$) and antisymmetrically ($|-\rangle_n$) shared between two adjacent atoms at a given lattice site n. The atomic interaction shifts their respective energies by $\pm J_L$. Therefore, the two atomic dimer states become energetically isolated for small L and separately generate reflection resonances at the collective energies $\tilde{\Delta}_\pm \sim \pm L^{-3}$, as indicated by the dashed lines in Fig. 1(a) [37]. Their respective widths are given by $\tilde{\Gamma}_\pm = \tilde{\Gamma}[1 \pm \cos(kL)]$, such that one finds an ultranarrow reflection resonance with $\tilde{\Gamma}_- \ll \tilde{\Gamma}$, generated by an effective array of subradiant atomic dimer states as L decreases.

For larger values of L, the evanescent-field coupling vanishes and the interaction between the arrays is predominantly generated by propagating photons. The coupling strength $J_L \approx 3\gamma\cos(kL)/kL$, therefore, acquires an oscillating behavior from the propagation phase and leads to an energy difference $\tilde{\Delta}_+ - \tilde{\Delta}_- \sim \sin(kL)$ that varies periodically with the array distance L. As both collective dimer states are excited by the parity-breaking incident field, their interference leads to a series of narrow transmission resonances, akin to electromagnetically induced transparency in three-level systems [37,38]. One can obtain a simple expression for the

dual-array transmission amplitude [37]

$$T = \frac{t^2}{1 - r^2 e^{2ikL}} \tag{4}$$

in terms of the reflection and transmission amplitudes, r and t, of the individual arrays. Substituting their explicit form, Eq. (3), we obtain the following condition for perfect transmission ($|T| = 1$),

$$\Delta - \tilde{\Delta} = -\tilde{\Gamma} \tan(kL), \tag{5}$$

that defines the series of transmission resonances. Along these resonances, transmitted photons can acquire a substantial group delay with a delay time [37]

$$\tau = \frac{2\tilde{\Gamma}}{(\Delta - \tilde{\Delta})^2}, \tag{6}$$

that diverges for resonant detunings $\Delta = \tilde{\Delta}$. The width of the transmission resonances decreases as $\sim 1/\tau$ around these values and, therefore, vanishes at $kL = n\pi$ for integer $n > 0$. In between the resonances ($kL = (n + 1/2)\pi$), the system features high reflection and behaves largely linear, which can be used to store several delocalized excitations across distant arrays at $L \gg \lambda$ [39].

Equation (4) describes the transmission of a Fabry-Pérot resonator composed of two identical mirrors with respective reflection and transmission amplitudes r and t. Here, however, the single-particle saturation of each emitter within the atomic mirrors together with the narrow subradiant transmission resonances can enhance optical nonlinearities and generate exceedingly strong photon-photon interactions.

We have studied the signatures of such photon-photon interactions via quantum trajectory wave function simulations [40] of the atomic master equation with Eqs. 1(a) and 1(b) for finite arrays. Working with finite arrays and focused driving beams generally entails photon losses that tend to broaden the otherwise ultranarrow transmission resonances. These effects can be mitigated through a proper choice of the atomic lattices, mathcing the wavefront profile of the incident beam [37,39]. In fact, already rather small lattices of 9×9 atoms permit to generate narrow transmission resonances with linewidths of $\sim 10^{-2}\gamma$ and high peak transmission of $|T| \sim 0.98$.

Figure 1(c) shows the calculated second order correlation function

$$g^{(2)}(t) = \frac{\langle \hat{E}^\dagger(t')\hat{E}^\dagger(t'+t)\hat{E}(t'+t)\hat{E}(t')\rangle}{\langle \hat{E}^\dagger(t')\hat{E}(t')\rangle^2} \tag{7}$$

of the transmitted light for an incident cw field with a Gaussian transverse beam profile whose waist is centered right in between the two arrays. We consider long times $t' \to \infty$, such that Eq. (7) yields the temporal photon-photon correlation in the steady state. Its dependence on the time delay, t, between consecutively detected photons indicates the generation of highly nonclassical light. Interestingly, one finds a rapid initial drop of the two-photon correlation function to small values $g^{(2)} \sim 0$, which extends over a broad range of delay times between two transmitted photons. These characteristic temporal correlations can be understood as follows. Let us denote the steady state of the two arrays as $|\psi\rangle$. Detection of a transmitted photon in the steady state then projects this state onto $|\bar{\psi}\rangle = \hat{E}|\psi\rangle/\sqrt{\langle\psi|\hat{E}^\dagger\hat{E}|\psi\rangle}$. The correlation function can thus be obtained as

$$g^{(2)}(t) = \frac{\langle \bar{\psi}(t'+t)|\hat{E}^\dagger\hat{E}|\bar{\psi}(t'+t)\rangle}{\langle \psi(t')|\hat{E}^\dagger\hat{E}|\psi(t')\rangle} \tag{8}$$

from the time evolved state $|\bar{\psi}(t'+t)\rangle$ following detection of a photon at time t'. For weak driving this state is predominantly determined by the collective ground state, $|0\rangle$, and the single-excitation manifold. It can hence be expressed as a superposition, $|\bar{\psi}\rangle = c_0|0\rangle + c_+|+\rangle + c_-|-\rangle$, of the collective superradiant ($|+\rangle$) and subradiant ($|-\rangle$) states of a single atomic excitation that is shared (anti)symmetrically across the two arrays, as discussed above. Indeed, the time evolution of the populations $|c_\pm|^2$ resembles the temporal photon correlations, see Fig. 2. The initial drop of $g^{(2)}$ thus reflects the fast decay of the superradiant excitation on a short timescale τ_+, leaving the dual array depleted of excitations. Its subsequent slow rise, on the other hand, can be traced back to the repopulation of the long-lived subradiant cavity state, $|-\rangle$, on a long timescale τ_- given by the inverse width of the transmission resonance, which corresponds to the photon delay time, discussed above (cf. Fig. 3(e), see [37]).

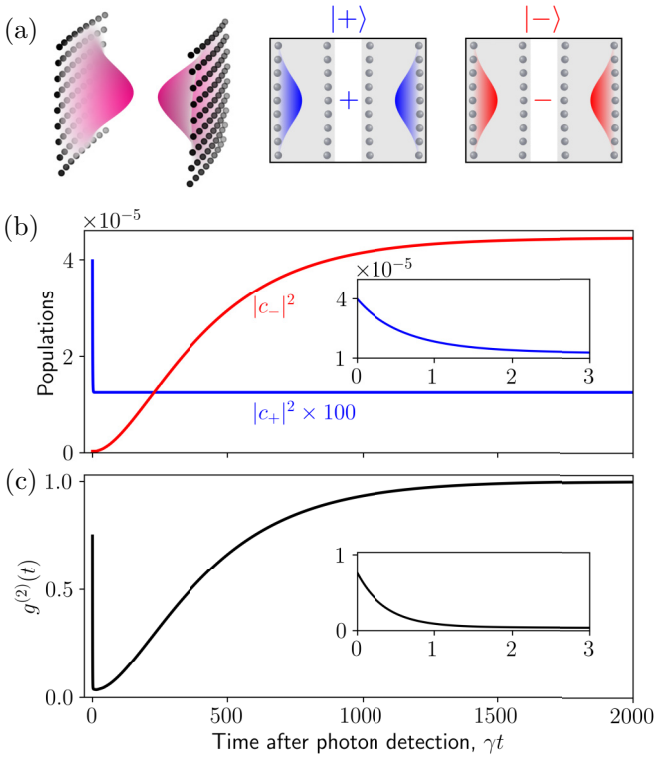

FIG. 2. (a) The characteristic time dependence of the two-photon correlation function, $g^{(2)}(t)$, can be understood by the dynamics of the shortlived ($|+\rangle$) and longlived ($|-\rangle$) single atomic excitation that is symmetrically ($|+\rangle$) and antisymmetrically ($|-\rangle$) delocalized between the two arrays. (b) Following the detection of a photon, the subsequent population dynamics, $|c_+|^2$ (blue) and $|c_-|^2$ (red), of these two states agrees with the characteristic time dependence of $g^{(2)}(t)$ shown in panel (c) (see text for more details). The parameters are the same as in Fig. 1(c).

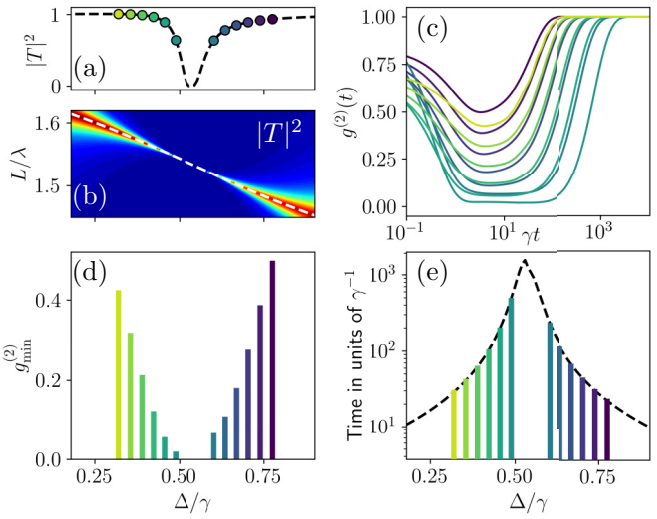

FIG. 3. (a) Transmission of a 9×9 dual array with the same parameters as in Fig. 1(a) along the transmission resonance marked by the white dashed line Figs. 1(a) and 1(b) and panel (b). (c) Two-photon correlation function, $g^{(2)}(t)$, at the different indicated points along this transmission resonance, as indicated by the color coding. Panel (d) shows the minimum value $g^{(2)}_{\min} = \min_t g^{(2)}(t)$. The color bars in panel (e) show the long timescale on which the correlation functions eventually approach unity, which matches the photon delay time, or photon confinement time, τ. Its asymptotic value for infinite arrays is given by Eq. (6), while the dashed line in panel (e) has been obtained numerically for the 9×9 arrays.

Consequently, we expect stronger effects of photon-photon interactions around more narrow transmission lines. This is demonstrated in Fig. 3, where we show the two-photon correlation function $g^{(2)}$ while scanning the frequency detuning, Δ, and the array distance, L, along the transmission maximum of one of the resonances, as illustrated in Fig. 3(b). Indeed, we find that the minimum value, $g^{(2)}_{\min} = \min_t g^{(2)}(t)$, of the two-photon correlation function decreases as the resonance becomes more narrow and the delay time increases. Owing to the finite size of the array, the linear transmission decreases as we approach this regime by varying L [Fig. 3(a)]. The associated losses tend to broaden the transmission lines and, as shown in Fig. 3(e), lead to a maximum delay time of $\tau \sim 1000/\gamma$, instead of the otherwise diverging behavior discussed above for infinite arrays and plane wave driving [cf. Eq. (6)]. Larger arrays yield longer photon confinement times, τ, for a given transmission maximum, which, therefore, enhances both the temporal extend and the strength of photon-photon correlations. Remarkably, however, one can reach large single-photon nonlinearities and highly nonclassical light with $g^{(2)}_{\min} \sim 0$ under conditions of high photon transmission already for moderate system sizes, which are achieved in ongoing optical lattice experiments [1,20].

We can gain further insights into the generated nonlinearity by considering the two-photon momentum density

$$\tilde{\rho}(\mathbf{k}_1, \mathbf{k}_2, t) = \langle \tilde{E}^\dagger(\mathbf{k}_1, t')\tilde{E}^\dagger(\mathbf{k}_2, t'+t)\tilde{E}(\mathbf{k}_2, t'+t)\tilde{E}(\mathbf{k}_1, t')\rangle \tag{9}$$

in the steady state ($t' \to \infty$), where $\tilde{E}(\mathbf{k}_\perp)$ is the transverse Fourier transform of the electric field operator of the transmitted light [37]. Figure 4 shows the in-plane momentum distribution of the two photons. In Figs. 4(a) and 4(b), we have fixed the transverse momentum $\mathbf{k}_1$ of one photon at the value indicated by the white star and show the equal-time momentum distribution of the other ($t = 0$). The distribution of $\mathbf{k}_2$ is sharply peaked around $-\mathbf{k}_1$ indicating that the optical nonlinearity can indeed be understood in terms of effective photon-photon collisions that preserve the total transverse momentum $\mathbf{k}_1 + \mathbf{k}_2 \simeq 0$ of the incident beam. Note that this approximate conservation law already emerges for moderate system sizes of 9×9 atoms. Figure 4(c) displays the equal-time momentum correlations between the y components of both photons for $k_{1,x} = k_{2,x} = 0$. The sharp maximum around $k_{2,y} = -k_{1,y}$ once more reflects the conservation of total momentum, while the variation along the antidiagonal results from the momentum dependence of the scattering process, i.e., the momentum dependence of the effective photon-photon interaction. The signal in the corners are due to Bragg scattering of the interacting photons.

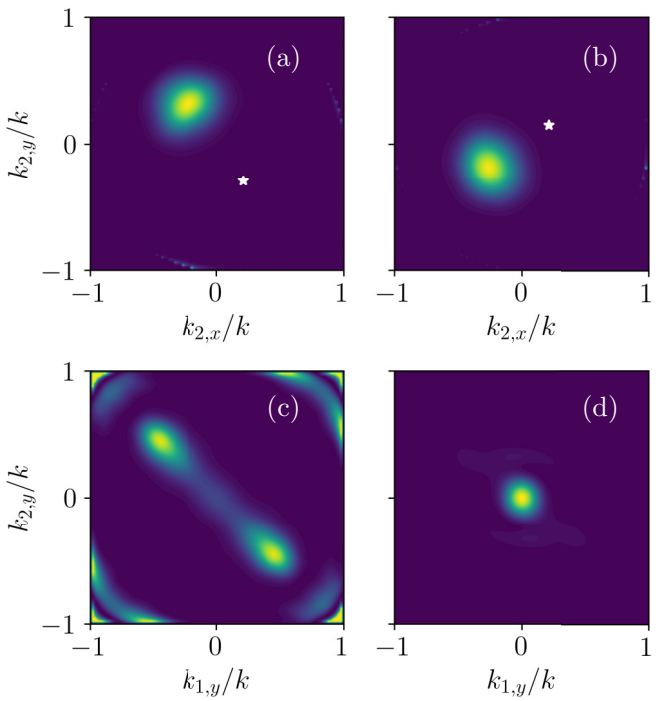

FIG. 4. (a) and (b) Momentum-space two-photon density $\tilde{\rho}(\mathbf{k}_1, \mathbf{k}_2, 0)$ for $\mathbf{k}_1\lambda = (1.33, -1.84)$, $(1.33, 0.95)$ respectively. The large density near $\mathbf{k}_1 + \mathbf{k}_2 \simeq 0$ shows the photons have scattered off each other with conserved momentum. (c) and (d) $\tilde{\rho}(\mathbf{k}_1, \mathbf{k}_2, t)$ for $k_{1,x} = k_{2,x} = 0$ with a time $t = 0$ and $t = 10/\gamma$, respectively, between the detection of the two photons. The time $t = 10/\gamma$ corresponds to $g^{(2)}(t) \sim 0$. Again, the antidiagonal bar in panel (c) indicates a momentum-conserving scattering among photons. After a time $t = 10/\gamma$ this correlation has vanished (see text for details). The color scheme is chosen such that each panel simply shows the qualitative structure. The system parameters are the same as in Fig. 1(c).

Figure 4(d) shows the same momentum density as in Fig. 4(c), but for a finite delay time $t = 10/\gamma$. In this case we observe practically no correlations in the transverse momenta and the signal corresponds to the transverse mode of the incident beam. This behavior can be readily understood

from the conditioned dynamics of the collective single excitation, discussed above (cf. Fig. 2). At small delay times, the two-photon signal naturally stems from the superradiant excitation following detection of the first photon. While the narrow linear transmission line arises from longlived subradiant excitations, the superradiant mode can only be populated by the interaction between multiple excitations. One therefore finds strong momentum correlations in the transverse two-photon signal, as shown in Figs. 4(a)–4(c) for a vanishing delay time $t = 0$. For longer delay times beyond the superradiant lifetime, the superradiant state is depleted and the second photon predominantly stems from the subradiant mode that is repopulated by the continuous optical driving of the arrays. The two detected photons, thus, originate from cascaded excitation and emission processes such that we find negligible transverse-momentum correlations, albeit strong temporal correlations, between the two photons. Despite the local nature of the underlying nonlinearity of each individual atom, this mechanism makes it possible to generate strongly correlated photons without significant transverse mode mixing in the plane of the atomic arrays.

Subwavelength lattices of ultracold atoms provide a promising platform for the coherent manipulation of optical fields, and in this work we have described how these perspectives can be extended into the domain of quantum nonlinear optics by using two atomic arrays. While large optical nonlinearities can also be generated in atomic ensembles via strong interactions between high-lying atomic Rydberg states [41–47], the present setting yields an alternative mechanism beyond the physics of excitation-blockaded superatoms. This is made possible by ultranarrow transmission resonances that emerge from interference between collective superradiant and subradiant states of the dual array, bearing analogies to electromagnetically induced transparency [38] and the physics of Fano resonators [48]. We have demonstrated that the single-photon saturation of each individual atom can generate a strong and finite-ranged effective interaction between photons. Such emerging photon-photon interactions suggest a number of questions for future work. We have identified a regime in which strong temporal photon correlations emerge under conditions of very low transverse-mode mixing, thus generating large nonlinearities for freely propagating single photonic modes at greatly suppressed losses. This motivates future explorations of applications as nonlinear quantum optical elements to generating and processing photonic quantum states [49–51], or to study the physics of propagating multiphoton quantum states [52–56] through a many of such nonlinear elements.

In this work, we have mainly focused on analyzing temporal correlations of photons in single transverse modes, drawing analogies to waveguide QED settings [23]. In addition, however, the multimode physics of large planar arrays should yield an interesting framework for exploring the many-body physics of multiple photons in the two-dimensional plane of the dual-array resonator, and motivates future work on the potential formation and nonlinear dynamics of effective cavity polaritons [31]. Hereby, our results indicate that this should make it possible to reach the quantum regime of strong interactions between individual polaritons.

We thank Kristian Knakkergaard, Aurélien Dantan, and Peter Rabl for valuable discussions. This work was supported by the Carlsberg Foundation through the Ardens" Research Project QCooL, and by the DNRF through the Center of Excellence" (Grant Agreement No. DNRF156).

[1] C. Gross and I. Bloch, Quantum simulations with ultracold atoms in optical lattices, Science **357**, 995 (2017).

[2] H. Zheng and H. U. Baranger, Persistent Quantum Beats and Long-Distance Entanglement from Waveguide-Mediated Interactions, Phys. Rev. Lett. **110**, 113601 (2013).

[3] J. D. Thompson, T. G. Tiecke, N. P. de Leon, J. Feist, A. V. Akimov, M. Gullans, A. S. Zibrov, V. Vuletić, and M. D. Lukin, Coupling a Single Trapped Atom to a Nanoscale Optical Cavity, Science **340**, 1202 (2013).

[4] J. Petersen, J. Volz, and A. Rauschenbeutel, Chiral nanophotonic waveguide interface based on spin-orbit interaction of light, Science **346**, 67 (2014).

[5] T. G. Tiecke, J. D. Thompson, N. P. de Leon, L. R. Liu, V. Vuletić, and M. D. Lukin, Nanophotonic quantum phase switch with a single atom, Nature (London) **508**, 241 (2014).

[6] A. Goban, C.-L. Hung, J. D. Hood, S.-P. Yu, J. A. Muniz, O. Painter, and H. J. Kimble, Superradiance for Atoms Trapped along a Photonic Crystal Waveguide, Phys. Rev. Lett. **115**, 063601 (2015).

[7] J. S. Douglas, H. Habibian, C.-L. Hung, A. V. Gorshkov, H. J. Kimble, and D. E. Chang, Quantum many-body models with cold atoms coupled to photonic crystals, Nat. Photonics **9**, 326 (2015).

[8] R. J. Coles, D. M. Price, J. E. Dixon, B. Royall, E. Clarke, P. Kok, M. S. Skolnick, A. M. Fox, and M. N. Makhonin, Chirality of nanophotonic waveguide with embedded quantum emitter for unidirectional spin transfer, Nat. Commun. **7**, 11183 (2016).

[9] G. Calajó, F. Ciccarello, D. Chang, and P. Rabl, Atom-field dressed states in slow-light waveguide QED, Phys. Rev. A **93**, 033833 (2016).

[10] H. Zoubi and K. Hammerer, Quantum Nonlinear Optics in Optomechanical Nanoscale Waveguides, Phys. Rev. Lett. **119**, 123602 (2017).

[11] A. Rosario Hamann, C. Müller, M. Jerger, M. Zanner, J. Combes, M. Pletyukhov, M. Weides, T. M. Stace, and A. Fedorov, Nonreciprocity Realized with Quantum Nonlinearity, Phys. Rev. Lett. **121**, 123601 (2018).

[12] S.-P. Yu, J. A. Muniz, C.-L. Hung, and H. J. Kimble, Two-dimensional photonic crystals for engineering atom–light interactions, Proc. Natl. Acad. Sci. USA **116**, 12743 (2019).

[13] Y. Ke, A. V. Poshakinskiy, C. Lee, Y. S. Kivshar, and A. N. Poddubny, Inelastic Scattering of Photon Pairs in Qubit Arrays with Subradiant States, Phys. Rev. Lett. **123**, 253601 (2019).

[14] R. Jones, G. Buonaiuto, B. Lang, I. Lesanovsky, and B. Olmos, Collectively Enhanced Chiral Photon Emission from an Atomic Array near a Nanofiber, Phys. Rev. Lett. **124**, 093601 (2020).

[15] R. J. Bettles, S. A. Gardiner, and C. S. Adams, Enhanced Optical Cross Section via Collective Coupling of Atomic Dipoles in a 2D Array, Phys. Rev. Lett. **116**, 103602 (2016).

[16] G. Facchinetti, S. D. Jenkins, and J. Ruostekoski, Storing Light with Subradiant Correlations in Arrays of Atoms, Phys. Rev. Lett. **117**, 243601 (2016).

[17] E. Shahmoon, D. S. Wild, M. D. Lukin, and S. F. Yelin, Cooperative Resonances in Light Scattering from Two-Dimensional Atomic Arrays, Phys. Rev. Lett. **118**, 113601 (2017).

[18] A. Asenjo-Garcia, M. Moreno-Cardoner, A. Albrecht, H. J. Kimble, and D. E. Chang, Exponential Improvement in Photon Storage Fidelities Using Subradiance and "Selective Radiance" in Atomic Arrays, Phys. Rev. X **7**, 031024 (2017).

[19] K. E. Ballantine and J. Ruostekoski, Optical Magnetism and Huygens' Surfaces in Arrays of Atoms Induced by Cooperative Responses, Phys. Rev. Lett. **125**, 143604 (2020).

[20] J. Rui, D. Wei, A. Rubio-Abadal, S. Hollerith, J. Zeiher, D. M. Stamper-Kurn, C. Gross, and I. Bloch, A subradiant optical mirror formed by a single structured atomic layer, Nature (London) **583**, 369 (2020).

[21] A. V. Poshakinskiy, J. Zhong, and A. N. Poddubny, Quantum Chaos Driven by Long-Range Waveguide-Mediated Interactions, Phys. Rev. Lett. **126**, 203602 (2021).

[22] T. L. Patti, D. S. Wild, E. Shahmoon, M. D. Lukin, and S. F. Yelin, Controlling Interactions between Quantum Emitters Using Atom Arrays, Phys. Rev. Lett. **126**, 223602 (2021).

[23] A. S. Sheremet, M. I. Petrov, I. V. Iorsh, A. V. Poshakinskiy, and A. N. Poddubny, Waveguide quantum electrodynamics: Collective radiance and photon-photon correlations, arXiv:2103.06824 [quant-ph] (2021).

[24] A. V. Kildishev, A. Boltasseva, and V. M. Shalaev, Planar photonics with metasurfaces, Science **339**, 1232009 (2013).

[25] N. Yu and F. Capasso, Flat optics with designer metasurfaces, Nat. Mater. **13**, 139 (2014).

[26] H.-T. Chen, A. J. Taylor, and N. Yu, A review of metasurfaces: Physics and applications, Rep. Prog. Phys. **79**, 076401 (2016).

[27] V.-C. Su, C. H. Chu, G. Sun, and D. P. Tsai, Advances in optical metasurfaces: fabrication and applications, Opt. Express **26**, 13148 (2018).

[28] C.-W. Qiu, T. Zhang, G. Hu, and Y. Kivshar, Quo vadis, metasurfaces?, Nano Letters, Nano Lett. **21**, 5461 (2021).

[29] A. Cidrim, T. S. do Espirito Santo, J. Schachenmayer, R. Kaiser, and R. Bachelard, Photon Blockade with Ground-State Neutral Atoms, Phys. Rev. Lett. **125**, 073601 (2020).

[30] L. A. Williamson, M. O. Borgh, and J. Ruostekoski, Superatom Picture of Collective Nonclassical Light Emission and Dipole Blockade in Atom Arrays, Phys. Rev. Lett. **125**, 073602 (2020).

[31] I. Carusotto and C. Ciuti, Quantum fluids of light, Rev. Mod. Phys. **85**, 299 (2013).

[32] C. Noh and D. G. Angelakis, Quantum simulations and many-body physics with light, Rep. Prog. Phys. **80**, 016401 (2017).

[33] This can be realized [20] by applying a sufficiently strong magnetic field to ensure that only one atomic transition is near-resonant with the incident driving field of a given polarization, and excitation exchange on other dipole transitions is energetically suppressed.

[34] R. H. Lehmberg, Radiation from an N -Atom System. I. General Formalism, Phys. Rev. A **2**, 883 (1970).

[35] M. Gross and S. Haroche, Superradiance: An essay on the theory of collective spontaneous emission, Phys. Rep. **93**, 301 (1982).

[36] A. Asenjo-Garcia, J. D. Hood, D. E. Chang, and H. J. Kimble, Atom-light interactions in quasi-one-dimensional nanostructures: A Green's-function perspective, Phys. Rev. A **95**, 033818 (2017).

[37] See Supplemental Material at http://link.aps.org/supplemental/10.1103/PhysRevResearch.5.L012047 for details on the linear response of the dual array, the effects of interactions between two arrays, group delay of transmitted photons, finite size effects, the numerical analysis of subradiant and superradiant states in finite dual arrays, and determining the E-field operator of a certain detection mode and the Fourier transform of the E-field.

[38] M. Fleischhauer, A. Imamoglu, and J. P. Marangos, Electromagnetically induced transparency: Optics in coherent media, Rev. Mod. Phys. **77**, 633 (2005).

[39] P.-O. Guimond, A. Grankin, D. V. Vasilyev, B. Vermersch, and P. Zoller, Subradiant Bell States in Distant Atomic Arrays, Phys. Rev. Lett. **122**, 093601 (2019).

[40] K. Mølmer, Y. Castin, and J. Dalibard, Monte Carlo wavefunction method in quantum optics, J. Opt. Soc. Am. B **10**, 524 (1993).

[41] M. Moreno-Cardoner, D. Goncalves, and D. E. Chang, Quantum nonlinear optics based on two-dimensional Rydberg atom arrays, Phys. Rev. Lett. **127**, 263602 (2021).

[42] L. Zhang, V. Walther, K. Mølmer, and T. Pohl, Photon-photon interactions in Rydberg-atom arrays, Quantum **6**, 674 (2022).

[43] Y. Solomons and E. Shahmoon, Multi-channel waveguide QED with atomic arrays in free space, arXiv:2111.11515 [quant-ph].

[44] T. Peyronel, O. Firstenberg, Q.-Y. Liang, S. Hofferberth, A. V. Gorshkov, T. Pohl, M. D. Lukin, and V. Vuletić, Quantum nonlinear optics with single photons enabled by strongly interacting atoms, Nature (London) **488**, 57 (2012).

[45] A. Paris-Mandoki, C. Braun, J. Kumlin, C. Tresp, I. Mirgorodskiy, F. Christaller, H. P. Büchler, and S. Hofferberth, Free-Space Quantum Electrodynamics with a Single Rydberg Superatom, Phys. Rev. X **7**, 041010 (2017).

[46] T. Stolz, H. Hegels, M. Winter, B. Röhr, Y.-F. Hsiao, L. Husel, G. Rempe, and S. Dürr, Quantum-Logic Gate between Two Optical Photons with an Average Efficiency above 40%, Phys. Rev. X **12**, 021035 (2022).

[47] J. Vaneecloo, S. Garcia, and A. Ourjoumtsev, Intracavity Rydberg Superatom for Optical Quantum Engineering: Coherent Control, Single-Shot Detection, and Optical π Phase Shift, Phys. Rev. X **12**, 021034 (2022).

[48] M. F. Limonov, M. V. Rybin, A. N. Poddubny, and Y. S. Kivshar, Fano resonances in photonics, Nat. Photonics **11**, 543 (2017).

[49] D. Witthaut, M. D. Lukin, and A. S. Sørensen, Photon sorters and QND detectors using single photon emitters, EPL **97**, 50007 (2012).

[50] T. C. Ralph, I. Söllner, S. Mahmoodian, A. G. White, and P. Lodahl, Photon Sorting, Efficient Bell Measurements, and a Deterministic Controlled- Z Gate Using a Passive Two-Level Nonlinearity, Phys. Rev. Lett. **114**, 173603 (2015).

[51] F. Yang, M. M. Lund, T. Pohl, P. Lodahl, and K. Mølmer, Deterministic Photon Sorting in Waveguide QED Systems, Phys. Rev. Lett. **128**, 213603 (2022).

[52] S. Mahmoodian, M. Čepulkovskis, S. Das, P. Lodahl, K. Hammerer, and A. S. Sørensen, Strongly Correlated Photon Transport in Waveguide Quantum Electrodynamics with Weakly Coupled Emitters, Phys. Rev. Lett. **121**, 143601 (2018).

[53] A. S. Prasad, J. Hinney, S. Mahmoodian, K. Hammerer, S. Rind, P. Schneeweiss, A. S. Sørensen, J. Volz, and A. Rauschenbeutel, Correlating photons using the collective nonlinear response of atoms weakly coupled to an optical mode, Nat. Photonics **14**, 719 (2020).

[54] S. Mahmoodian, G. Calajó, D. E. Chang, K. Hammerer, and A. S. Sørensen, Dynamics of Many-Body Photon Bound States in Chiral Waveguide QED, Phys. Rev. X **10**, 031011 (2020).

[55] O. A. Iversen and T. Pohl, Strongly Correlated States of Light and Repulsive Photons in Chiral Chains of Three-Level Quantum Emitters, Phys. Rev. Lett. **126**, 083605 (2021).

[56] O. A. Iversen and T. Pohl, Self-ordering of individual photons in waveguide QED and Rydberg-atom arrays, Phys. Rev. Res. **4**, 023002 (2022).